Structure and Properties of Injection Moldings of Polypropylene/Polystyrene Blends

MITSUYOSHI FUJIYAMA

Plastics Research Laboratory, Tokuyama Corp., Tokuyama-shi, Yamaguchi-ken 745, Japan

Received 13 March 1996; accepted 1 July 1996

ABSTRACT: A homoisotactic polypropylene (PP) was melt blended with 0–30 wt % of three kinds of polystyrene (PS) with melt flow indexes lower than, similar to, and higher than that of PP. The blends were injection molded at cylinder temperatures of 200–280°C, and the structure and properties of the injection moldings were studied. With PS blending, although the PP molding whitened, no surface defect such as layer peeling and pearl-like appearance occurred. The rigidity and dimensional accuracy of the molding improved without much deterioration in impact strength and heat resistance. At the same time the fluidity also improved. The injection moldings of PP/PS blends did not show clear skin/core structure under a polarizing microscope. The degrees of crystallinity and crystalline c-axis orientation decreased with PS blending. PS particles were the smallest when the ratio of the viscosity of the PS to that of PP at molding shear rate was slightly lower than unity. © 1997 John Wiley & Sons, Inc. J Appl Polym Sci **63:** 1015–1027, 1997

INTRODUCTION

Many authors have investigated the structure and properties of injection-molded polypropylenes (PPs) and studied the effects of molding conditions,[1] molecular weight,[2–5] copolymerization with ethylene,[6,7] addition of α-crystal nucleators,[8,9] addition of β-crystal nucleators,[10–12] particulate filling,[13–16] and glass fiber filling.[17] In the present study, the structure and properties of injection moldings of PP/polystyrene (PS) blends were investigated in order to study the effect of the polymer blend.

The literature on the studies of structure and properties of PP/PS blends and injection-molded PP blends are surveyed in this article. Shimizu et al.[18,19] studied the melt spinning of PP/PS blends and reported on the morphology and formation mechanism of ultrafine fibrils[18] and their orientation behavior and mechanical properties.[19] They reported that by PS blending, the amount of a*-axis oriented crystals increase in proportion and the degree of orientation and amount of c-axis oriented crystals decrease. Kakizaki[20,21] polymerized styrene in the presence of PP and developed a new polymer alloy (Mitsubishi Yuka VMX) in which PS particles disperse more uniformly and finely in PP matrix than those in simple PP/PS blends. Because PS reacts to PP at the interface in this polymer alloy, it shows less negative deviation from additivity of the flexural modulus versus the composition than simple blends and hence has superior impact strength. Gupta and Purwar[22] reported that PP blended with 10 wt % PS shows a slightly higher modulus and impact strength than PP while the tensile strength and elongation markedly decrease. Mucha[23] presumed that there is an interaction between PP and PS because the glass transition temperature of PS increases and the glass transition temperature and melting point of PP decrease when PS is blended with PP. Wenig and colleagues[24] studied the crystallization

dynamics of PP/PS blends and showed that although the density of crystal nuclei decreases with increasing PS content, the growth rate of PP spherulites scarcely changes. Iwata et al.[25,26] reported that the PP phases in PP/PS blends mixed by use of a screw extruder are microfibrillar and the fibrillation of the PP phase is notable when the viscosity of the PP is lower than that of the PS. Hlavatá and Horák[27] studied the WAXS and SAXS of a PP blended with a high impact PS (HIPS) and showed that although the crystallinity of PP in a simple PP/HIPS blend scarcely changes from PP, it slightly decreases when styrene-butadiene (SB) or styrene-butadiene-styrene (SBS) block copolymer is added as a third component.

Next, studies on injection molding of PP blends are reviewed. Thamm[28] injection molded PP/ethylene-propylene-diene terpolymer (EPDM) blends and showed that the EPDM domains in the skin layer are larger than those in the core layer and orients in the flow direction. Furthermore, he showed that the weld part is weak because the EPDM particles at the weld part orient perpendicular to the flow direction and parallel to the weld plane and form thin sheets. Asar and coworkers[29] showed that the skin layers in injection-molded PP/EPDM blends are thicker than that in injection-molded PP. Salovey et al.[30] showed that the EPDM particles in the skin layer in an injection-molded PP/PS blend are elongated lengthwise in the flow direction when fractured parallel to the flow direction and form ellipsoids when fractured perpendicular to the flow direction. They also showed that the EPDM particles in the core layer are spherical. Karger–Kocsis[31] showed that the EPDM particles in the skin layers in injection-molded PP/EPDM blends are elongated flatly parallel to the flow direction and that the degree of elongation becomes weaker on going away from the surface. Vongdars and cohorts[32] showed that an injection-molded PP/LDPE blend exhibits a clear skin/core structure in the whole composition range and that the skin layer becomes thicker with decreasing injection speed, cylinder temperature, and mold temperature. Fisa et al.[33] showed that the polycarbonate (PC) particles in injection-molded PP/PC (0–40 vol %) blends are spherical or ellipsoidal in the core layer and elongated in sheetlike form in the flow direction in the skin layer at low PC contents and that the PC phases are elongated fibrously parallel to the flow direction in both the skin and core layers at a high PC content of 40 vol %. They also showed that the yield stress and tensile modulus are additive in spite of the incompatibility of PP and PC. D'Orazio and colleagues[34] showed that the ethylene-propylene rubber (EPR) particles in the core layer in an injection-molded PP/EPR blend become smaller when decreasing the ratio of viscosity of the EPR to that of PP. Lee and Chen[35] showed that an injection-molded PP/polyburene (PB)-1 blend exhibits a skin/core structure in the whole composition range and that the skin layer becomes thinner with increasing PB-1 content. Furthermore, they reported that although the tensile modulus and yield strength monotonously decrease with increasing PB-1 content, the ultimate elongation and strength show synergisms at PB-1 contents of 25 and 50 vol %. Michaeli et al.[36] showed that the degree of orientation of PP molecular chains in injection-molded PP/EPDM blends is lower than that in an injection-molded PP. They also showed that the variation in the thickness direction of the degree of elongation in the flow direction of the EPDM particles is very similar to that of the degree of molecular chain orientation.

In the present study, the blends of amorphous PS to crystalline PP were selected as an ideal incompatible blend. A PP was melt blended with three kinds of PSs with melt flow indexes (MFIs) higher than, similar to, and lower than that of PP. The blends were injection molded at cylinder temperatures of 200–280°C, and the structure and properties of injection moldings were studied.

As far as the author knows, no study on the structure and properties of an injection-molded PP/PS blend has been reported up to this time.

EXPERIMENTAL

Samples

The PP (a homoisotactic PP) that was used was Tokuyama Polypro Grade ME140, with an MFI of 8.0 g/10 min (Tokuyama Corp.).

The PS (atactic PSs) that were used were ESTYRENE G-12-15 (MFI at 200°C, 5000 g = 2.5 g/10 min, abbreviated as PSL), G-20 (MFI = 9.5 g/10 min, PSM), and G-32 (MFI = 31.0 g/10 min, PSH), which were produced by Nippon Steel Chemical Co., Ltd.

Figure 1 shows the temperature changes of the MFIs (230°C, 2160 g, converted on PP volume) of the PP and PSs. PSL had a lower MFI than PP at all temperature ranges; PSH had a higher MFI

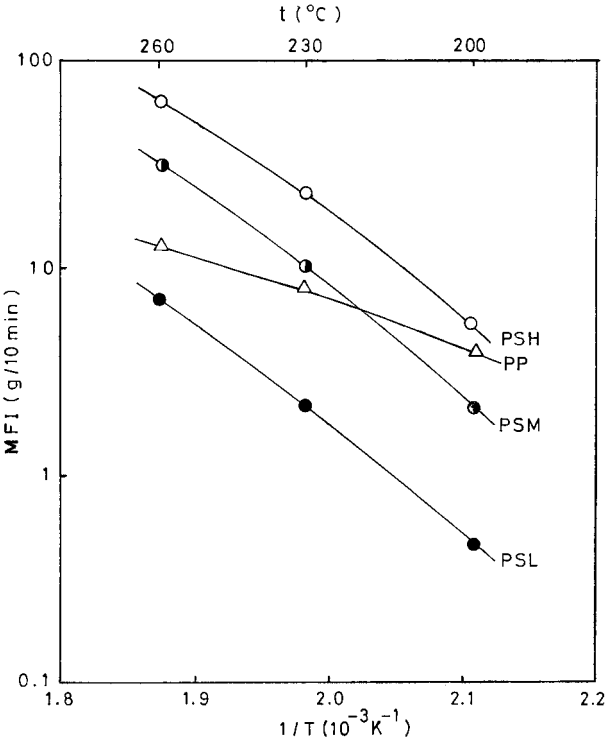

Figure 1 Temperature changes of MFIs of raw resins.

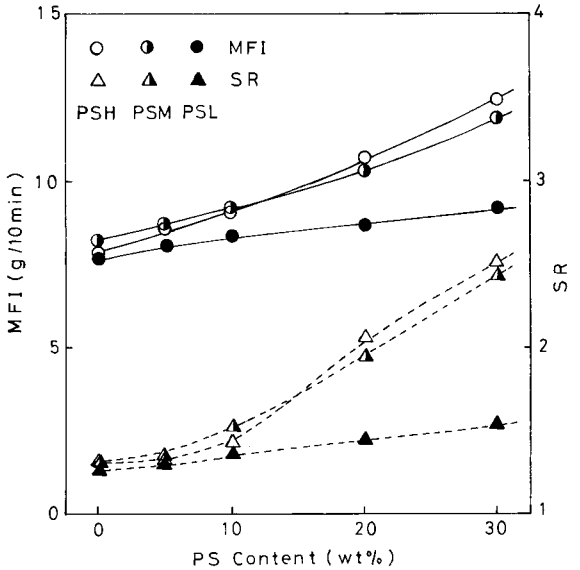

Figure 2 Dependence of MFI and die swell ratio, SR, of blends on PS content.

than PP at all temperature ranges, and PSM had lower and higher MFIs than PP at temperatures below and above 230°C, respectively.

The PP was thoroughly mixed with requisite amounts of the PSs and extruded by a 40-mm diameter extruder with a Dulmage screw at 240°C. Extrudates were cut into pellets of about 3-mm size by a pelletizer. PS contents were 0, 5, 10, 20, and 30 wt %. A sample with PS content of 0 was also pelletized under the same conditions. [Hereafter the PP/PS blends will be abbreviated as each PS (PSL, PSM, PSH) followed by a hyphen and PS content.]

Figure 2 shows the dependence of the MFI (230°C, 2160 g, converted on PP volume) and die swell ratio (SR = D/D_o; D, diameter of extrudate; D_o, diameter of orifice) on PS content. The MFI of the PP/PS blend increased with increasing PS content for all the PSs including PSL with a lower MFI than PP, indicating that PPs blended with PS show a high fluidity. The high fluidity of PP/PS blends was assumed to be caused by slipping at the interface between the PP and PS phases at the time of flowing because of the incompatibility of both components. The SR of the PP/PS blend increased with increasing PS content. The increase of SR was especially notable when PSH or PSM was blended by the amounts of 20 wt % or more. It is a general fact that the SRs of polymer blends are higher than those of the components.

Figure 3 shows, as an example, the dependence of crystallization temperature, T_c, and latent heat of crystallization, ΔH_c, of the PP/PSM system on PSM content, which were measured by a differential scanning calorimeter (DSC, Seiko Electronic Industry DSC-200). A sheet 0.3 mm thick was molded on a hot plate. It was put into a DSC sample pan and melted in a furnace in a nitrogen atmosphere at 230°C for 10 min, followed by cooling at a rate of 10°C/min. The peak temperature and area of the exothermic curve were taken as T_c and ΔH_c, respectively. T_c decreased rapidly with

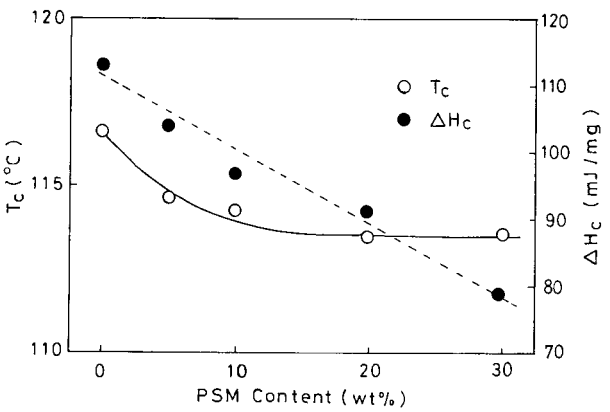

Figure 3 Dependence of crystallization temperature, T_c, and latent heat of crystallization, ΔH_c, on PS content (PSM system).

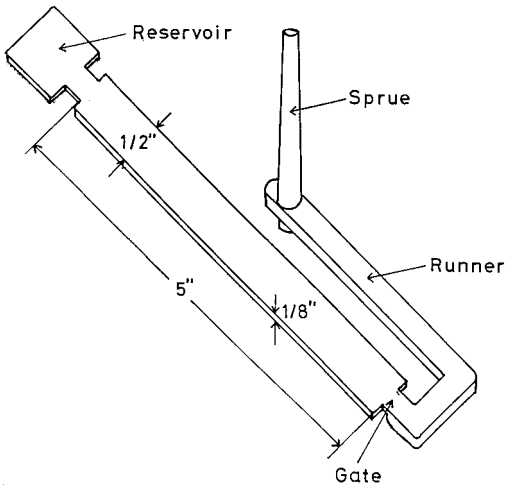

Figure 4 Shape of flexural test specimen.

increasing PSM content up to 10 wt % and tended to level off at PSM contents above 10 wt %. ΔH_c decreased almost linearly with increasing PSM content. For PSL and PSH systems, both T_c and ΔH_c decreased almost linearly with increasing PS content. From the fact that the T_c of PP decreased by PS blending, it was assumed that there was an interaction between PP and PS as reported by Mucha.[23] The decrease of ΔH_c by PS blending was slightly lower than the theoretical value.

Injection Molding

Flexural (ASTM D790) and notched Izod (ASTM D256) test specimens were injection molded using a 6.5-oz SN150S-N type reciprocating-screw injection molding machine produced by Niigata Tekkosho Co., Ltd. The shape of the flexural test specimen is shown in Figure 4. A reservoir at the end of the cavity was designed to reduce the end effect. The Izod test specimen had a notch of $r = 0.25$ mm and depth of 2.54 mm at one side of the center of a 5-in. part of the flexural test specimen. Because the cylinder temperature among molding conditions most strongly affects the degree of orientation and mechanical properties of the molded article,[1] injection molding was carried out, varying only the cylinder temperature and keeping other conditions constant. The injection molding conditions are shown in Table I. The cylinder temperatures were represented by the temperature of the metering zone (C_3) at the extreme end.

Measurement of Properties

After flexural and Izod test specimens were conditioned under a constant 23°C temperature and 50% relative humidity (RH) for 17–20 days, flexural modulus and flexural strength were measured with a Shimadzu Autograph AG-5000A according to ASTM D790. Heat distortion temperature was measured under a constant stress of 0.45 MPa according to ASTM D648. Izod impact strength was measured with molded-in notched specimens according to ASTM D259. Length, L, in the machine direction (MD) of the flexural specimen was measured with a micrometer and mold shrinkage was calculated by the following equation:

$$\text{mold shrinkage}\ (\%) = \frac{L_o - L}{L_o} \times 100, \quad (1)$$

where L_o is the length of the mold cavity.

Structural Analyses

Thin sections about 20 μm thick were sliced from the central parts of the flexural test specimens perpendicular to the flow direction (MD) with a microtome, and their crystalline textures were ob-

Table I Injection Molding Conditions

Exp. No.	Cylinder Temperature (°C) C_1[a]	C_2[b]	C_3[c]	C_4[d]	Injection Speed (cm^3/s)	Injection Pressure (MPa)	Mold Temperature (°C)	Injection Time (s)	Cooling Time (s)
1	160	190	200	190	13.5	50	40	30	10
2	160	220	240	220	13.5	50	40	30	10
3	160	250	280	250	13.5	50	40	30	10

[a] Feed zone.
[b] Compression zone.
[c] Metering zone.
[d] Nozzle.

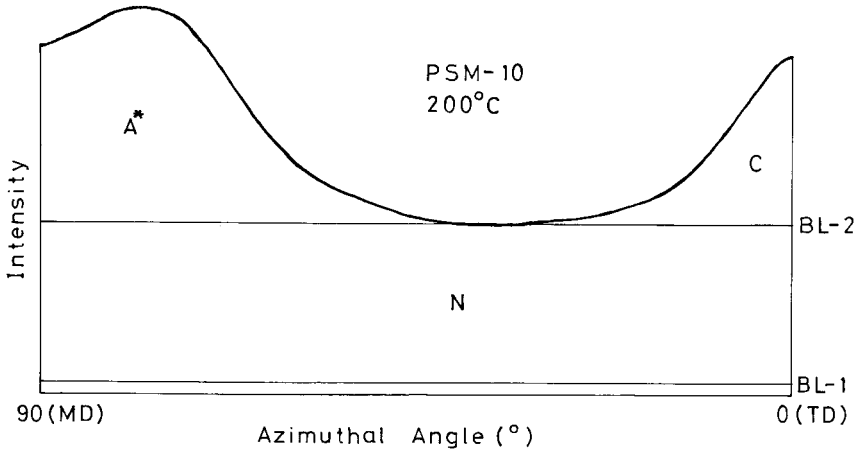

Figure 5 Azimuthal scan curve of (110) plane reflection of wide-angle X-ray diffraction (PSM-10, 200°C).

served with a polarizing microscope (Olympus BH-2) under a magnification of 20×.

Scan (2θ) wide-angle X-ray diffractograms were measured in the through direction at the central parts of the flexural specimens with a Rigaku Denki RU-200 Diffractometer with Ni-filtered Cu-K_α radiation using a rotating specimen table, which rotates the specimen at a speed of 90 rpm and compensates the orientation effect. The crystallinities, X_c, were obtained according to the method of Weidinger and Hermans.[37] Using a goniometer, 2θ scans and azimuthal scans of the (110) and (040) plane reflections were carried out in the through direction on the same specimens as used for the crystallinity measurement. The crystalline c-axis orientation functions, f_c, were calculated according to the Wilchinsky method.[38]

Figure 5 exemplifies the (110) plane azimuthal scan curve of a specimen molded from a PSM-10 sample at a cylinder temperature of 200°C. Here, in order to evaluate the proportions of the c-axis oriented component and a^*-axis oriented component, the following procedure was carried out: a baseline (BL2) was drawn horizontally at the bottom of the azimuthal scan curve; the area around an azimuthal angle of 0° above the BL2 was taken as C and the area around an azimuthal angle of 90° above the BL2 was taken as A^*; the a^*-axis oriented component fraction $[A^*]$ was defined as follows:

$$[A^*] = \frac{A^*}{C + A^*} . \qquad (2)$$

Furthermore, a quantity OF (orientation fraction) was used as a measure of crystalline orientation and was defined as follows:

$$\mathrm{OF} = \frac{C + A^*}{C + A^* + N} , \qquad (3)$$

where N (nonoriented) is the area enveloped by the BL2 and BL1, which is the baseline of the 2θ scan curve.

The fracture surfaces of the Izod test specimens were observed with a scanning electron microscope (SEM; JEOL JSM-T220) under a magnification of 2000×, and the dispersion states of the PS particles were studied. Diameters of 100 PS particles in the SEM photographs were measured and number averaged to obtain the average diameter d_n. The d_n was obtained for each sample molded at each cylinder temperature. Finally, the d_n of PSL-5, PSL-10, PSL-20, and PSL-30 samples molded at one cylinder temperature were averaged; and the average d_n of the PSL system molded at that cylinder temperature was obtained. Likewise, the average d_n of the PSL system molded at other cylinder temperatures were obtained. In the same manner, the average d_ns of other PS systems molded at each cylinder temperature were obtained.

Measurement of Viscosity

Apparent viscosity versus apparent shear rate curves of PP and PSs were measured with a capillary rheometer (Capirograph 1B, Toyoseiki Seisakusho C., Ltd.) at temperatures of 200, 240, and 280°C, which were in accord with the cylinder temperatures in injection molding. The die used had dimensions of length L = 5 mm, radius $2R$ = 0.5 mm, and L/R = 20. Apparent viscosity versus apparent shear rate curves of the PP/PS

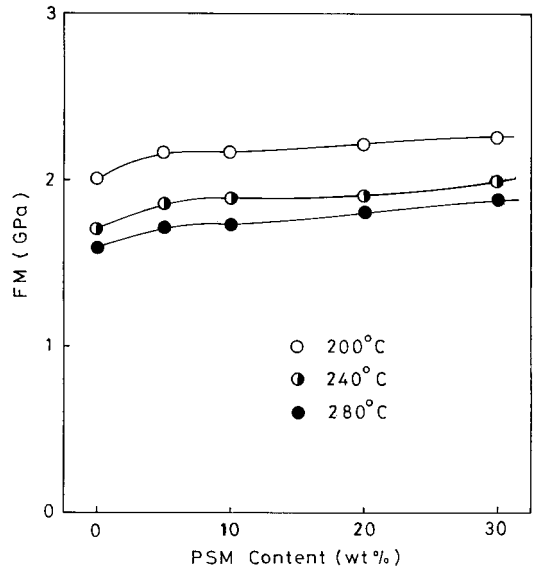

Figure 6 Dependence of flexural modulus, FM, on PS content and cylinder temperature (PSM system).

blends were measured using the same die at a temperature of 240°C.

RESULTS AND DISCUSSION

Properties

Figure 6 exemplifies the dependence of flexural modulus, FM, on the PS content and cylinder temperature for the PSM system. FM was higher as the cylinder temperature was lowered and increased by PSM blending. The increase was particularly notable at PSM contents of up to 5 wt % and slight at PSM contents above 5 wt %. The effect of kind (MFI) of PS was scarcely observed.

As an example, Figure 7 shows the dependence

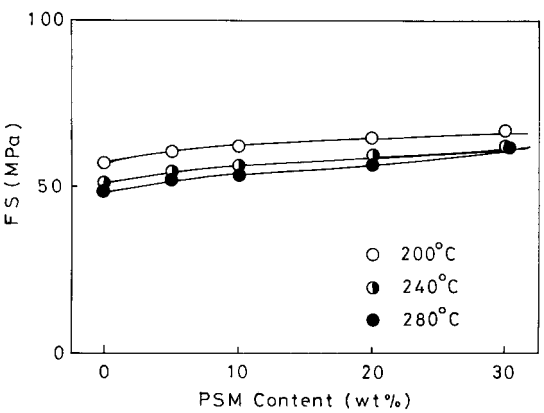

Figure 7 Dependence of flexural strength, FS, on PS content and cylinder temperature (PSM system).

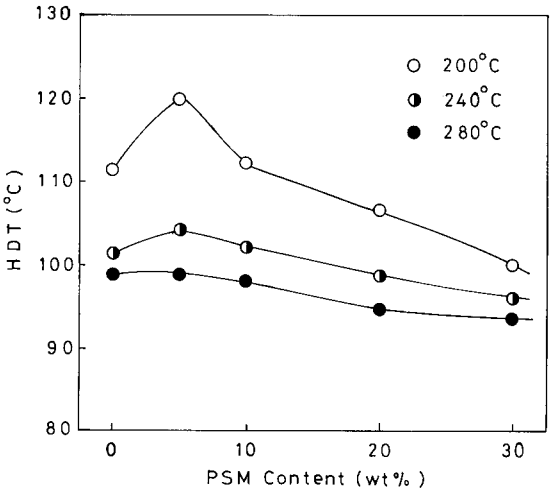

Figure 8 Dependence of heat distortion temperature, HDT, on PS content and cylinder temperature (PSM system).

of flexural strength, FS, on the PS content and cylinder temperature for the PSM system. As in the case of FM, FS was higher as the cylinder temperature was lowered and increased by PSM blending. The tendency of the notable increase in FS at PSM contents of up to 5 wt %, which was observed for FM, was slight for FS. The effect of the MFI of the PS was scarcely observed.

Figure 8 shows the dependence of heat distortion temperature, HDT, on the PS content and cylinder temperature for the PSM system. HDT rose as the cylinder temperature was lowered and showed a maximum at a PSM content of around 5 wt % at low cylinder temperatures (200 and 240°C). The reason why HDT showed a maximum at a PSM content of around 5 wt % is not obvious at the present time and further studies are needed. HDT monotonously decreased with increasing PSM content at the high cylinder temperature (280°C). The effect of the MFI of the PS was scarcely observed.

The dependence of Izod impact strength, IIS, on the PS content and cylinder temperature for the PSM system is shown in Figure 9. Although there was a tendency for the IIS to show a maximum at a PSM content of around 5 wt % at a cylinder temperature of 200°C, it may be said that IIS was scarcely changed by PSM blending as a whole. The reason why IIS showed a maximum at a PSM content of around 5 wt % is not clear at the present time. There was a tendency for IIS to be higher as the cylinder temperature was lowered. The effect of the MFI of the PS was scarcely observed.

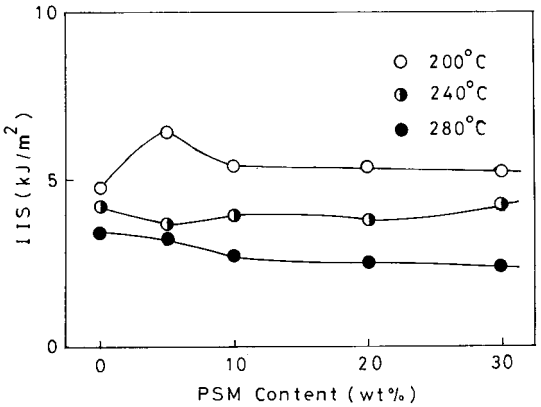

Figure 9 Dependence of Izod impact strength, IIS, on PS content and cylinder temperature (PSM system).

Figure 10 shows the dependence of mold shrinkage, MS, on the PS content and cylinder temperature for the PSM system. MS decreased as the cylinder temperature increased and was decreased by PSM blending. MS decreased slightly at PSM contents of up to 5 wt % and decreased rapidly after that. From this fact it can be said that the dimensional accuracy of injection-molded PP was improved by PS blending. The effect of the MFI of the PS was scarcely observed.

Apparent flow curves of the PSM system are shown in Figure 11. Although the viscosities of PP and PSM were scarcely different, the viscosity of PP was decreased by PSM blending.

From the above results, it may be said that

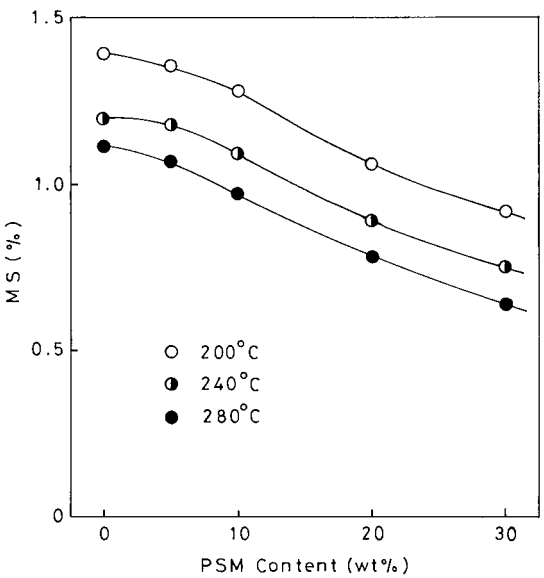

Figure 10 Dependence of mold shrinkage, MS, on PS content and cylinder temperature (PSM system).

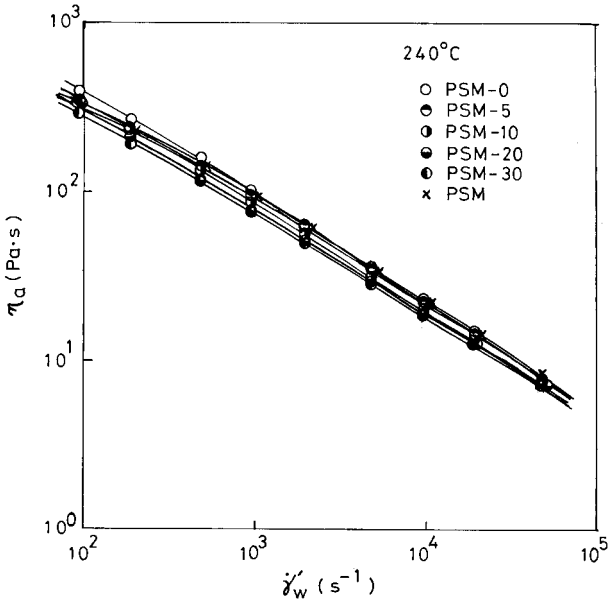

Figure 11 Apparent flow curves (PSM system; 240°C; die, L = 5 mm, $2R$ = 0.5 mm, L/R = 20).

the rigidity and dimensional accuracy of injection-molded PP are improved by PS blending without much deterioration of impact strength and heat resistance. In addition, the fluidity at molding is also improved by PS blending as shown in Figures 2 and 11.

Structural Analysis

Although an injection molding of PP not containing PS is translucent, it is whitened by PS blending. However, no surface defect such as layer peeling and pearl-like brightness was observed on any injection moldings of PP/PS blends in this experiment.

The change of crystalline texture observed under a polarizing microscope with the cylinder temperature for the PSM system is exemplified in Figure 12. The injection molding of PSM-0, which did not contain PSM, showed a clear skin/core structure. The thickness of the skin layer decreased with increasing cylinder temperature. However, the skin/core structure in an injection molding of the sample that contained even 5 wt % of PSM became obscure and the boundary between the skin and core layers was not clear. The PSL and PSH systems also showed similar behavior, and the skin/core structure in an injection molding of PP blended with PS was obscure.

Figure 13 shows, as an example, the dependence of crystallinity X_c on the PS content and

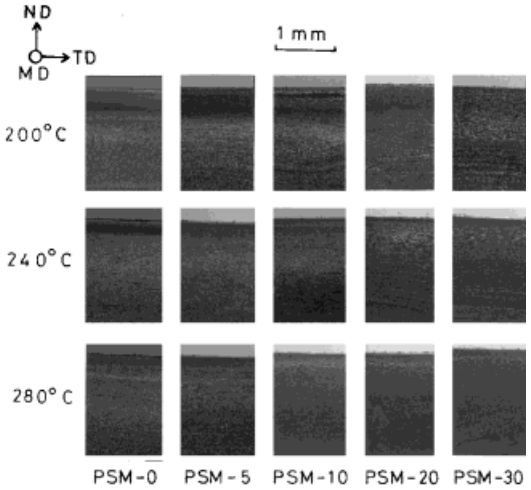

Figure 12 Change of crystalline texture observed with polarizing microscope with PS content and cylinder temperature (PSM system).

cylinder temperature for the PSM system. X_c decreased with increasing PSM content and was scarcely affected by the cylinder temperature. The decrease in X_c with increasing PSM content was particularly notable at PSM contents of up to 5 wt %. Such a tendency scarcely depended on the kind (MFI) of PS. If it is supposed that the PS component was contained in the amorphous region, the decrease in X_c with increasing PS content was slightly lower than that of the theoretical value.

The dependence of crystalline c-axis orientation function f_c on the PS content and cylinder temperature for the PSM system is illustrated in Figure 14; f_c was lowered as the cylinder temperature was raised and linearly decreased with increasing PSM content. Such a tendency scarcely depended on the MFI of the PS. From this fact it was surmised that the crystalline orientation of the injection-molded PP was decreased by PS blending. The fact that the crystalline orientation of injection-molded PP was decreased by EPDM blending was reported by Michaeli et al.[36] Furthermore, the fact that the crystalline orientation of melt-spun PP fiber was decreased by PS blending was reported by Shimizu and colleagues.[19] It was not clear that the decrease of crystalline orientation of injection-molded PP by PS blending was caused by the difficulty of melt orientation at the time of flow in the cavity, the short relaxation time of the melt orientation, or the long time before crystallization. (The crystallization temperature T_c was decreased by PS blending as shown

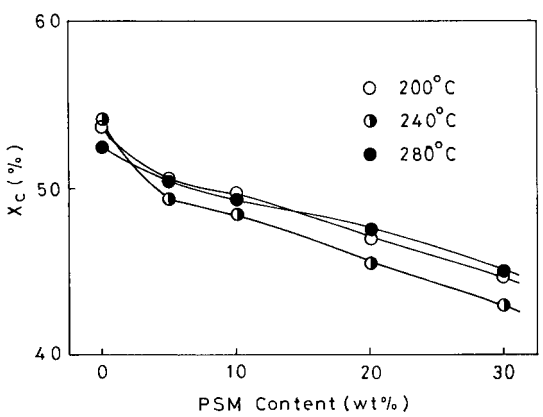

Figure 13 Dependence of crystallinity, X_c, on PS content and cylinder temperature.

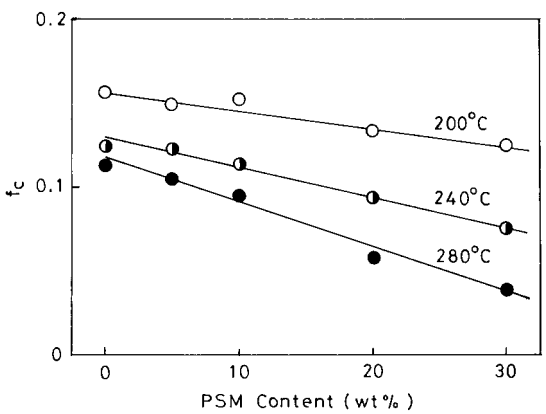

Figure 14 Dependence of crystalline c-axis orientation function, f_c, on PS content and cylinder temperature (PSM system).

in Fig. 3.) However, it seemed that the three causes were all possible. The fact that FM and FS increased with increasing PS content, as shown previously, suggests that the increase of rigidity by PS blending was superior to the decrease of rigidity caused by the decrease in the orientation of the PP. There is no correspondence between the maxima of the HDT and the IIS at a PS content of around 5 wt % at low cylinder temperatures, and the crystalline orientation (f_c) and hence the former cannot be explained by the latter. It was assumed that the decrease of the MS by the PS blending was caused both by the decrease in molecular orientation and by the low MS of the PS itself.

Figure 15 shows the dependence of crystalline orientation fraction OF on the PS content and cylinder temperature for the PSM system. OF was higher as the cylinder temperature was lowered. OF increased with increasing PSM content and tended to level off at PSM contents of 10–20 wt % at a cylinder temperature of 200°C. It showed a maximum at PSM contents of 10 and 5 wt % at cylinder temperatures of 240 and 280°C, respectively. This tendency scarcely depended on the MFI of the PS. It may be said that the crystalline c-axis orientation function f_c is a measure of the degree of orientation of crystalline molecular chains and that the crystalline orientation fraction OF is a measure of the amount of oriented crystals; f_c decreased linearly and OF increased as a whole with increasing PS content as shown before. From these facts it can be posited that while the mean degree of orientation of PP crystals decreased with increasing PS content, the amount of oriented crystals increased with increasing PS content. The skin/core structure was not clear in injection moldings of PP/PS blends under a polarizing microscope as shown in Figure 12. However, if the skin layer existed, its degree of molecular orientation might have been decreased by PS blending while its thickness might have been increased by PS blending.

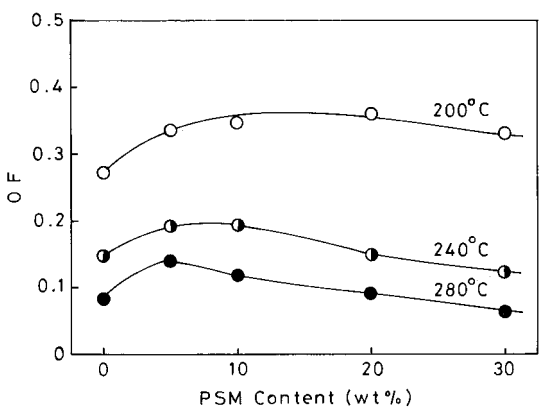

Figure 15 Dependence of crystalline orientation fraction, OF, on PS content and cylinder temperature (PSM system).

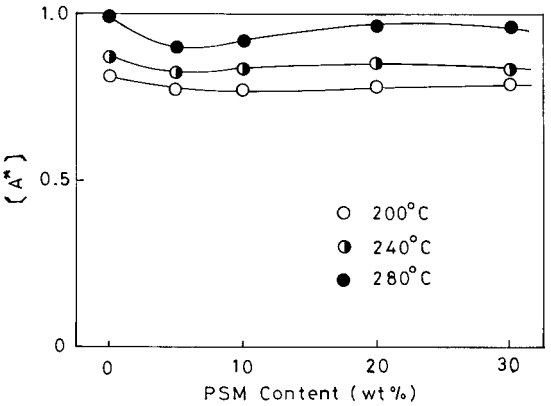

Figure 16 Dependence of a*-axis oriented fraction, [A*], on PS content and cylinder temperature (PSM system).

The dependence of the a*-axis oriented component fraction [A*] on the PS content and cylinder temperature for the PSM system is shown in Figure 16. [A*] was higher as the cylinder temperature was increased and decreased by PSM blending. This tendency hardly depended on the MFI of the PS. Shimizu et al.[19] reported that the [A*] of a melt-spun PP fiber was increased by PS blending, which is the inverse tendency of the present experiment. This reason is not clear at the present time.

The SEM photographs in Figure 17 show the changes of the fracture surface of the core part of the IIS specimen with the PS content and cylinder temperature. For the PSL system in which PSL with an MFI higher than that of PP was blended, the size of the PSL particles increased with increasing PSL content and decreased with increasing cylinder temperature. For the PSM system in which PSM with an MFI similar to that of PP was blended, the size of the PSM particles increased with increasing PSM content and was the smallest at a cylinder temperature of 240°C. The PSH system in which PSH with an MFI higher than that of PP was blended showed a similar change to the PSM system. According to Wu,[39] the dispersed particle size in a polymer blend becomes smaller as the shear rate at processing increases, the interfacial tension between the dispersoid and me-

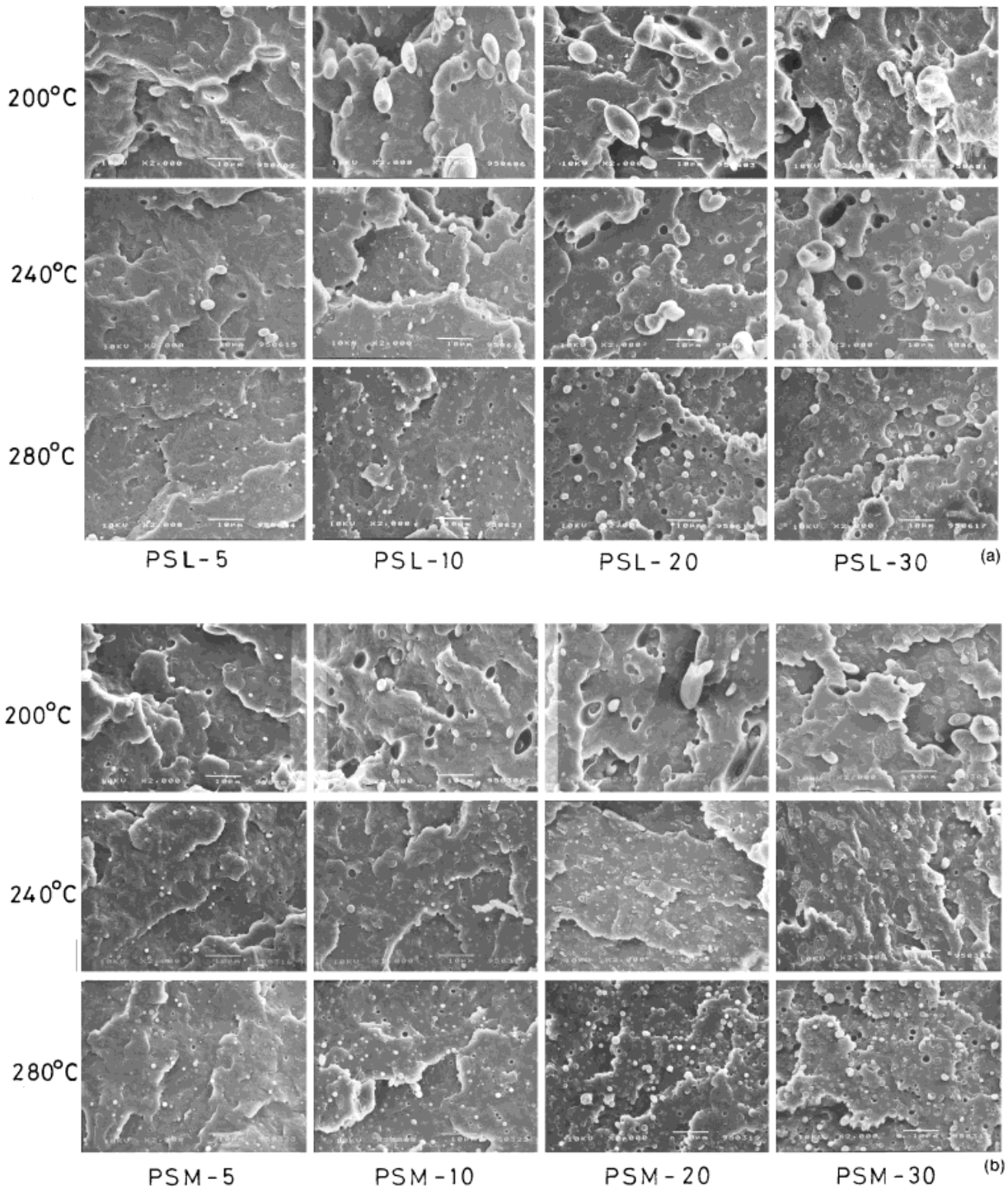

Figure 17 Change of SEM photograph of fracture surface of Izod impact test specimen with PS content and cylinder temperature; (a) PSL system, (b) PSM system, (c) PSH system.

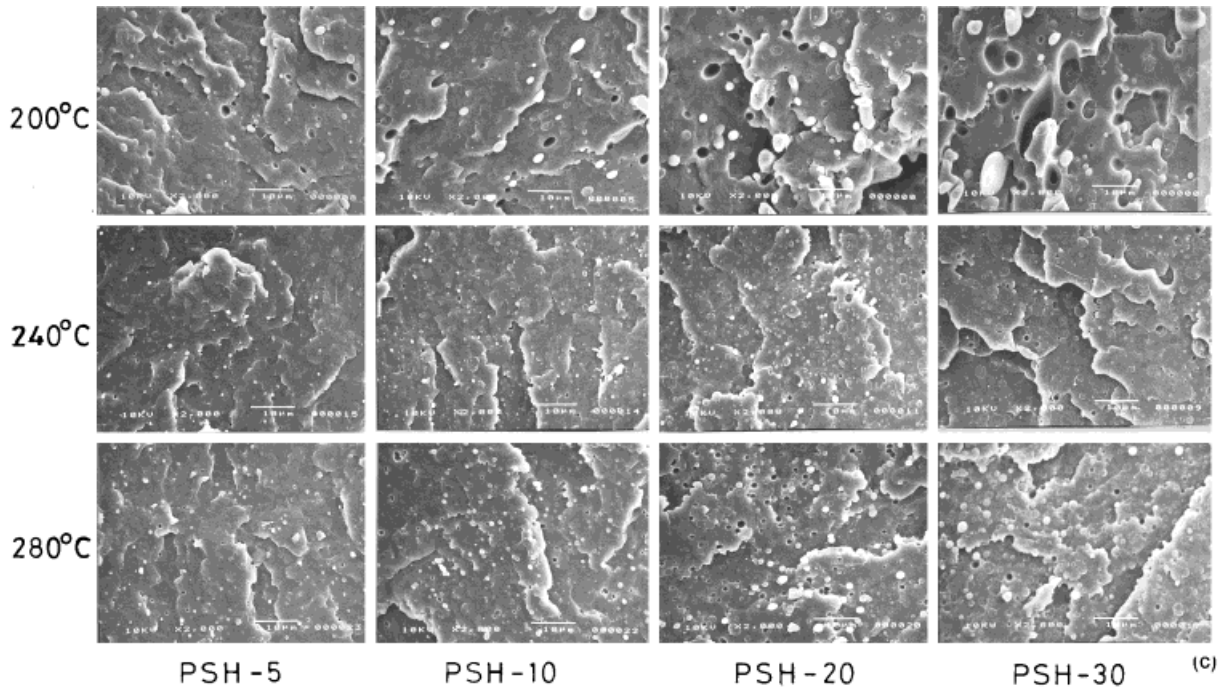

Figure 17 *(Continued from the previous page)*

dium becomes small, and the ratio of viscosity of the dispersoid to that of the medium at processing becomes unity. In the present experiment, the shear rate at processing and the interfacial tension were constant and only viscosity ratio at processing differed. Accordingly, the viscosity of each raw material was measured. The shear rate $\dot{\gamma}'_w$ at the gate of the mold cavity used in this experiment (Fig. 4) was calculated from the dimension of the gate and injection speed to be 4200 s^{-1}. Then the viscosity η_a at the shear rate $\dot{\gamma}'_w = 4200$ s^{-1} was obtained; its temperature dependence (Arrhenius plot) is shown in Figure 18. For PSL the viscosity was higher than that of PP at all temperature ranges, the viscosity ratio approaching unity with increasing temperature. For PSM the viscosity was similar to that of PP at 240°C; the former was higher than the latter at 200°C; and the former was lower than the latter at 280°C. For PSH the viscosity was higher than that of PP at 200°C; the former was slightly lower than the latter at 240°C; and the former was much lower than the latter at 280°C.

The relationship between the number-average particle size d_n and the viscosity ratio η_{PS}/η_{PP} is demonstrated in Figure 19. The value of d_n of each point in this figure is the average of d_ns of specimens with PS contents of 5, 10, 20, and 30 wt %. The PS particle size was large when the ratio of the viscosity of the PS to that of the PP was higher or lower than unity, and it was the smallest when the viscosity ratio was slightly lower than unity.

CONCLUSIONS

A PP was melt blended with 0–30 wt % of three kinds of PSs with MFIs lower than, similar to, and

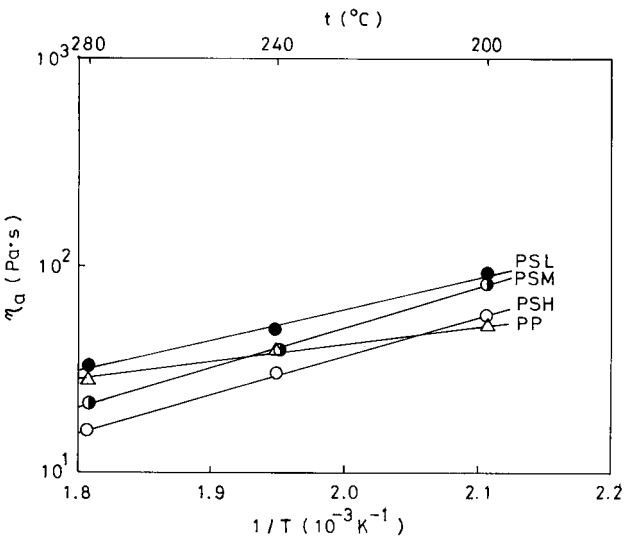

Figure 18 Temperature change of apparent viscosity, η_a, at apparent shear rate $\dot{\gamma}'_w = 4200$ s^{-1}.

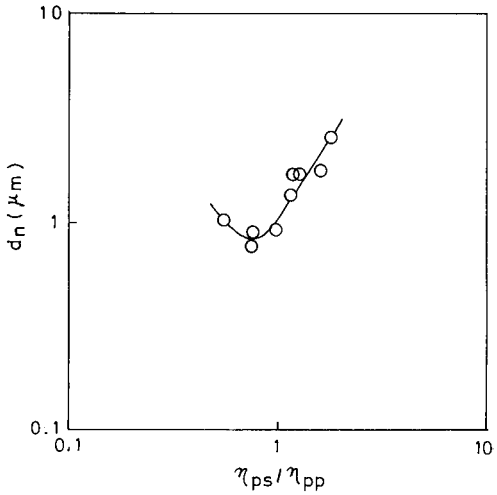

Figure 19 Relationship between number-average particle diameter, d_n, and viscosity ratio η_{PS}/η_{PP}.

higher than that of PP. The blends were injection molded at cylinder temperatures of 200–280°C, and the structure and properties of the injection moldings were studied.

1. The crystallization temperature and latent heat of crystallization decreased almost linearly with increasing PS content, which suggests an interaction between PP and PS.
2. Although the PP molding was whitened by PS blending, no surface defect such as layer peeling and pearl-like brightness appeared.
3. The flexural modulus and strength were higher as the cylinder temperature was lowered and were slightly increased by PS blending.
4. The HDT increased as the cylinder temperature was decreased and showed a maximum at a PS content of 5 wt % at low cylinder temperatures. It decreased with increasing PS content at high cylinder temperature.
5. The IIS rose as the cylinder temperature declined. Although it tended to show a maximum at a PS content of 5 wt % at low cylinder temperature, it was scarcely changed by PS blending as a whole.
6. The mold shrinkage was lower as the cylinder temperature was higher and was decreased by PS blending.
7. The fluidity was increased by PS blending.
8. Injection moldings of PP/PS blends did not show a clear skin/core structure under a polarizing microscope.
9. The crystallinity of injection molding of the PP/PS blend decreased almost linearly with increasing PS content.
10. The crystalline c-axis orientation of an injection molding of a PP/PS blend decreased almost linearly with increasing PS content.
11. The crystalline orientation fraction increased and the a^*-axis oriented component fraction decreased with increasing PS content.
12. PS particles were large when the ratio of viscosity of the PS to that of the PP was higher or lower than unity and were the smallest when the viscosity ratio was slightly lower than unity.

The author would like to thank Tokuyama Corp. for permission to publish this article.

REFERENCES

1. M. Fujiyama and S. Kimura, *Kobunshi Ronbunshu,* **32,** 581 (1975).
2. M. Fujiyama and S. Kimura, *J. Appl. Polym. Sci.,* **21,** 2283 (1977).
3. M. Fujiyama and S. Kimura, *J. Appl. Polym. Sci.,* **21,** 1225 (1978).
4. M. Fujiyama, *Nihon Reoroji Gakkaishi,* **14,** 152 (1986).
5. M. Fujiyama and T. Wakino, *J. Appl. Polym. Sci.,* **43,** 57 (1991).
6. M. Fujiyama and T. Wakino, *Int. Polym. Process.,* **7,** 97 (1992).
7. M. Fujiyama and T. Wakino, *Int. Polym. Process.,* **7,** 159 (1992).
8. M. Fujiyama and T. Wakino, *J. Appl. Polym. Sci.,* **42,** 2739 (1991).
9. M. Fujiyama and T. Wakino, *J. Appl. Polym. Sci.,* **42,** 2749 (1991).
10. M. Fujiyama, *Int. Polym. Process.,* **10,** 172 (1995).
11. M. Fujiyama, *Int. Polym. Process.,* **10,** 251 (1995).
12. M. Fujiyama, *Int. Polym. Process.,* to appear.
13. M. Fujiyama, Y. Kawasaki, and T. Wakino, *Nihon Reoroji Gakkaishi,* **15,** 191 (1987).
14. M. Fujiyama, Y. Kawasaki, and T. Wakino, *Nihon Reoroji Gakkaishi,* **15,** 203 (1987).
15. M. Fujiyama and T. Wakino, *J. Appl. Polym. Sci.,* **43,** 97 (1991).
16. M. Fujiyama, *Int. Polym. Process.,* **7,** 158 (1992).
17. M. Fujiyama, *Int. Polym. Process.,* **8,** 245 (1993).
18. J. Shimizu, N. Okui, T. Yamamoto, M. Ishii, and A. Takaku, *Sen-i Gakkaishi,* **38,** T-1 (1982).
19. J. Shimizu, N. Okui, T. Yamamoto, M. Ishii, and A. Takaku, *Sen-i Gakkaishi,* **38,** T-153 (1982).
20. T. Kakizaki, *Plast. Age,* **June,** 117 (1984).

21. T. Kakizaki, *SPE Tech. Paper 43rd ANTEC,* **31,** 934 (1985).
22. A. K. Gupta and S. N. Purwar, *J. Appl. Polym. Sci.,* **30,** 1799 (1985).
23. M. Mucha, *Colloid Polym. Sci.,* **264,** 859 (1986).
24. W. Wenig, H.-W. Fiedel, and A. Scholl, *Colloid Polym. Sci.,* **268,** 528 (1990).
25. I. Iwata, M. Yoshimura, Y. Ishida, K. Tanaka, and T. Ueki, *Polym. Prepr. Jpn.,* **39,** 3599 (1990).
26. I. Iwata, M. Yoshimura, Y. Ishida, K. Tanaka, and T. Ueki, *Mech. Behav. Mater.,* 295 (1992).
27. D. Hlavatá and Z. Horák, *Eur. Polym. J.,* **30,** 597 (1994).
28. R. C. Thamm, *Rubber Chem. Technol.,* **50,** 24 (1977).
29. H. K. Asar, M. B. Rhodes, and R. Salovey, *Adv. Chem. Ser.,* **176,** 489 (1979).
30. R. Salovey, W.-J. Ho, A. Nader, and A. J. Chompff, *ACS Polym. Prepr.,* **20,** 516 (1979).
31. J. Karger–Kocsis, *Polym. Eng. Sci.,* **27,** 241 (1987).
32. B. Vongdars, I. D. Simonov–Emel'yanov, V. N. Kuleznev, M. L. Katsevman, and N. V. Yuzvak, *Int. Polym. Sci. Technol.,* **17**(5), T/67 (1990).
33. B. Fisa, B. D. Favis, and S. Bourgeois, *Polym. Eng. Sci.,* **30,** 1051 (1990).
34. L. D'Orazio, C. Mancarella, E. Martuscelli, and F. Polato, *Polymer,* **32,** 1186 (1991).
35. M.-S. Lee and S.-A. Chen, *Polym. Eng. Sci.,* **33,** 686 (1993).
36. W. Michaeli, M. Cremer, and R. Bluhm, *Kunststoffe,* **83,** 992 (1993).
37. W. Weidinger and P. H. Hermans, *Makromol. Chem.,* **50,** 98 (1961).
38. Z. Wilchinsky, *J. Appl. Phys.,* **31,** 1969 (1960).
39. S. Wu, *Polym. Eng. Sci.,* **27,** 335 (1987).